Approach to Side Force Alleviation Through Modification of the Pointed Forebody Geometry

V. J. Modi* and A. C. Stewart†
University of British Columbia, Vancouver, British Columbia, V6T 1Z4 Canada

Aerodynamics of a circular cylinder with conical-shaped forebodies is studied at a subcritical Reynolds number of around 10^5. Attention is primarily focused upon modification of the forebody geometry to minimize the side force coefficient at high angles of attack. The tip geometries used are the standard cone, a family of nose booms, a set of delta strakes, porous tips, spinning nose-boom tips, and their combinations. The effectiveness of each tip in reducing the side force is assessed over a range of flight conditions and compared with the standard tip data. The results suggest that such tip modifications can reduce the side force in the range of 50-88%.

Nomenclature

A_b = base area of cone, $\pi D^2/4$
A_R = aspect ratio
C_N = coefficient of normal force, normal force/$(q \cdot A_b)$
C_P = coefficient of pressure, P/q
C_S = coefficient of side force, side force/$(q \cdot A_b)$
D = cone base diameter
L = total cone length
L_b = nose-boom length
L_s = strake length
P, P_∞ = local and reference freestream static pressures, respectively
q = freestream dynamic pressure head, $(1/2)\rho V_\infty^2$
Re = Reynolds number, $\rho V_\infty D/\mu$
V, V_∞ = local and freestream velocities, respectively
α = angle of attack
β = yaw angle
δ = cone half-angle
θ = angular position in role with respect to a fixed reference frame
μ = dynamic viscosity
ρ = density
ϕ = angular circumferential position of a pressure tap

I. Introduction

COMBAT agility requirements for current and the next generation of fighter airplanes have emphasized the need for controlled flight capability to increasingly high angles of attack. V/STOL type of configurations under study for a variety of military as well as civilian missions, including intercity commuter traffic, also use high attitude takeoff and descent. Such aircraft commonly employ pointed forebody fuselage. The boundary-layer separation leading to helical vortices, asymmetric both in strength and location, has often resulted in an undesirable side force, of uncertain direction, and the associated yawing moment. It is generally accepted that asymmetric character of the wake is promoted by the freestream turbulence and microscopic disparity of surface roughness distribution near the apex of the forebody.

It is important to recognize that besides fuselage of the high performance airplanes, tip tanks, bombs, missiles, launch vehicles, hubs of propellers, etc., also present pointed forebody geometries. Normally, such a pointed forebody configuration is incorporated as a part of the streamlined structure to reduce drag, increase stability, and aid in generating lift. Although a simple cone geometry is sometimes used, a more common pointed forebody is a tangent ogive or its variations.

The onset of significant side force occurs at an angle of attack approximately equal to the apex angle and at its peak can be of the same order of magnitude as the lift generated by the forebody. On aircraft this would correspond to an angle of attack when the rudder is partially shadowed by the wake of the fuselage. This may lead to the situation where the side force is an order of magnitude larger than the correcting force available from the rudder.

A study concerning variation of the lift and drag coefficients with the angle of attack for four models with the same cylindrical base but different conical forebodies showed[1] the maximum lift coefficient (C_L) of about 3.6 to be associated with the forebody having the smallest cone angle (20 deg) and occurred at $\alpha = 55$ deg. The corresponding C_D (drag coefficient) was 4.6 (Fig. 1). It is significant that the same model showed the maximum side force coefficient of 3.95. Symbols are explained in the diagram.

This being the case, the fluid dynamics of slender pointed bodies at high angles of attack has been a topic of long-standing interest to fluid dynamicists. A vast body of literature has accumulated over years touching upon different aspects of the problem, including pressure and force field distribution, wake structure, vortex breakdown, numerical prediction of the process, and, above all, mechanisms for alleviation of the side force. Three excellent papers by Ericsson and Reding[2-4] go a long way in briefing an interested researcher on the status of the subject. A paper by Modi et al.[1] and the recent thesis by Stewart[5] review the literature at some length.

However, the rate at which the new literature continues to appear is truly astonishing. It also suggests importance attached to the subject matter with reference to evolution of the next generation of high performance airplanes. Current focus appears to be on understanding physical parameters contributing to vortex asymmetry and its control as suggested by highly informative investigations of Moskovitz et al.,[6,7] Tavella et al.,[8] Hoang et al.,[9] Blake and Barnhart,[10] and Zilliac et al.[11] Furthermore, considerable efforts are directed toward numerical simulation of the complex flow[12-15] and, in some cases, assessment as to the effectiveness of the procedure through comparison with reliable experimental data.[16,17] Of equal importance has been the unique in-flight flow visualization study

Presented as Paper 90-2834 at the AIAA Atmospheric Flight Mechanics Conference, Portland, OR, Aug. 20-22, 1990; received Nov. 30, 1990; revision received April 12, 1991; accepted for publication April 12, 1991.

*Professor, Department of Mechanical Engineering. Fellow AIAA.
†Graduate Research Assistant, Department of Mechanical Engineering; currently Captain, Canadian Air Forces.

and its comparison with ground-based data as reported by Del Frate and Zuniga.[18]

With this as background, the paper presents results of an extensive test program aimed at assessing effectiveness of several passive and semiactive tip devices in reducing side force at high angles of attack in subsonic incompressible flows. These include 1) a family of nose booms with different lengths, 2) a set of delta strakes, 3) porous tips, and 4) spinning nose-boom tips and their combinations. The results obtained with the standard cone tip are also included to facilitate comparison.

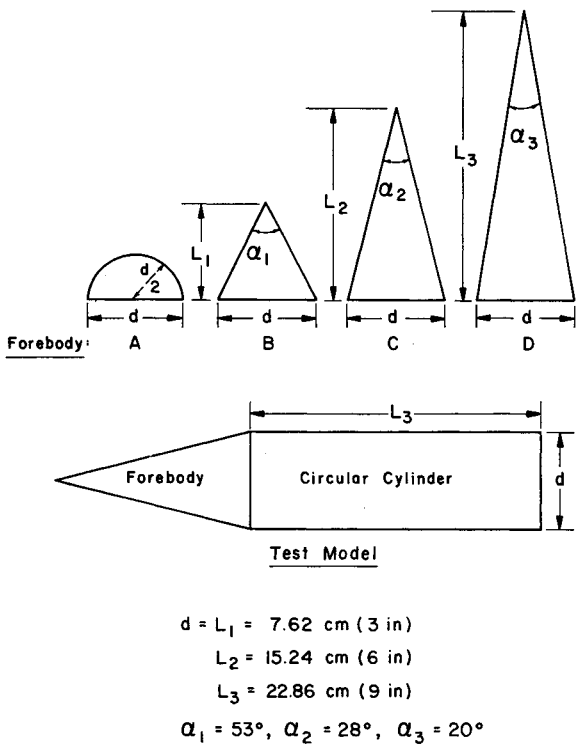

Fig. 1a Four tip geometries used to assess the effect of apex angle on lift and drag coefficients.

II. Model and Test Arrangement

Cone-Cylinder Model

For the entire experimental program, a cylindrical base, 7 cm in diameter and 10 cm long, with a conical forebody, formed the basic test model. The hollow aluminum cone with an apex angle of ≈ 28 deg was 15.25 cm (6 in.) long and had a base diameter of 7.82 cm (3 in.). It accommodated up to 40 pressure taps. The static pressure at a tap, typically 0.64 mm in diameter, is conveyed by a polyethylene tube, 1.7-mm inside diameter, to an externally located pressure transducer. The apex of the cone can be separated at two locations to replace it with desired tip geometries. The cylindrical aftbody housed a variable speed dc motor to rotate the tip at a controlled speed during one phase of the experimental program. The aftbody was also connected to a yoke-type vertical support, in turn mounted on the wind-tunnel balance platform, such that the angle of attack and yaw inclinations could be adjusted as required.

To minimize the effect of the surface roughness on the boundary-layer instability and, hence, better identify the influence of tip geometry on the side force, the cone model was provided with a smooth mirror finish. With the exception of the nose tips, the entire model was polished to within 5–7 μ surface roughness. As the objective of the study is to assess the effectiveness of the tip geometry in reducing the side force, microasymmetries at the tip were purposely retained to help simulate the real-life situation. The tests focused primarily on a family of delta strakes, nose booms, porous tips, and their combinations. Of course, the standard conical tip was also tested extensively to provide base information for comparison. A schematic diagram of the cone model and tip geometries tested is shown in Fig. 2.

It may be pointed out that a literature review suggests that both the nose boom and delta strake affect the side force.[1,3,19,20] The nose-boom lengths used in the experiments varied from 0.16 to 2.7 cm (aspect ratio variation based on the maximum boom diameter corresponded to 2 and 46, respectively). The span of the delta strake varied from 0.32 to 3.2 cm with an aspect ratio of 2. As several investigators[3,6,20,21] have reported a loss of lateral-directional stability with the delta strake, the tests were also conducted in the yaw angle range of ±10 deg.

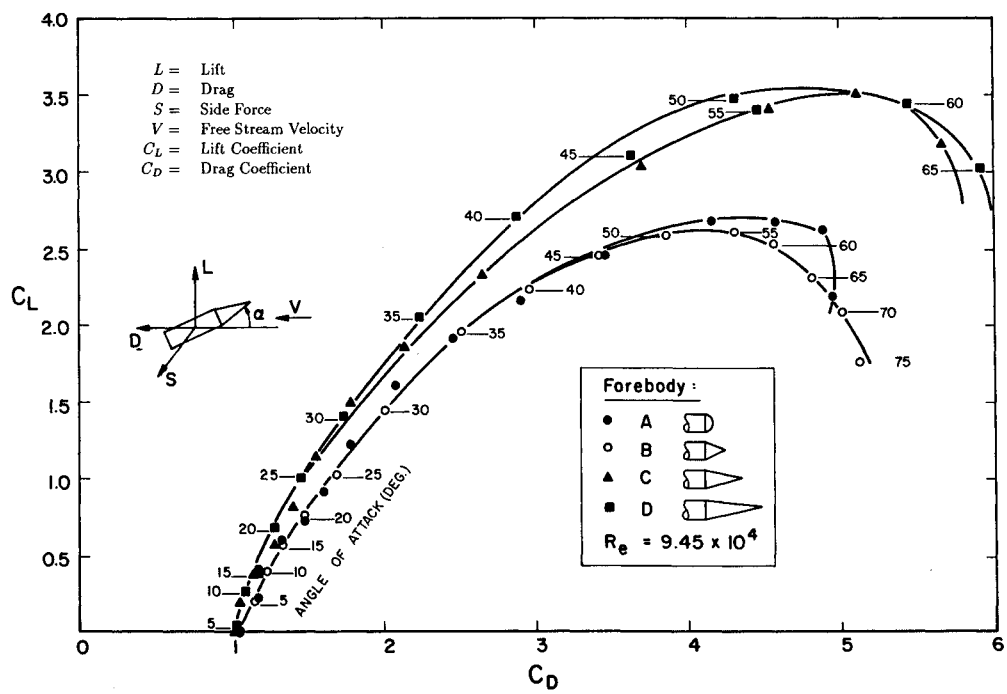

Fig. 1b Variation of lift and drag coefficients as functions of angle of attack for the four models.

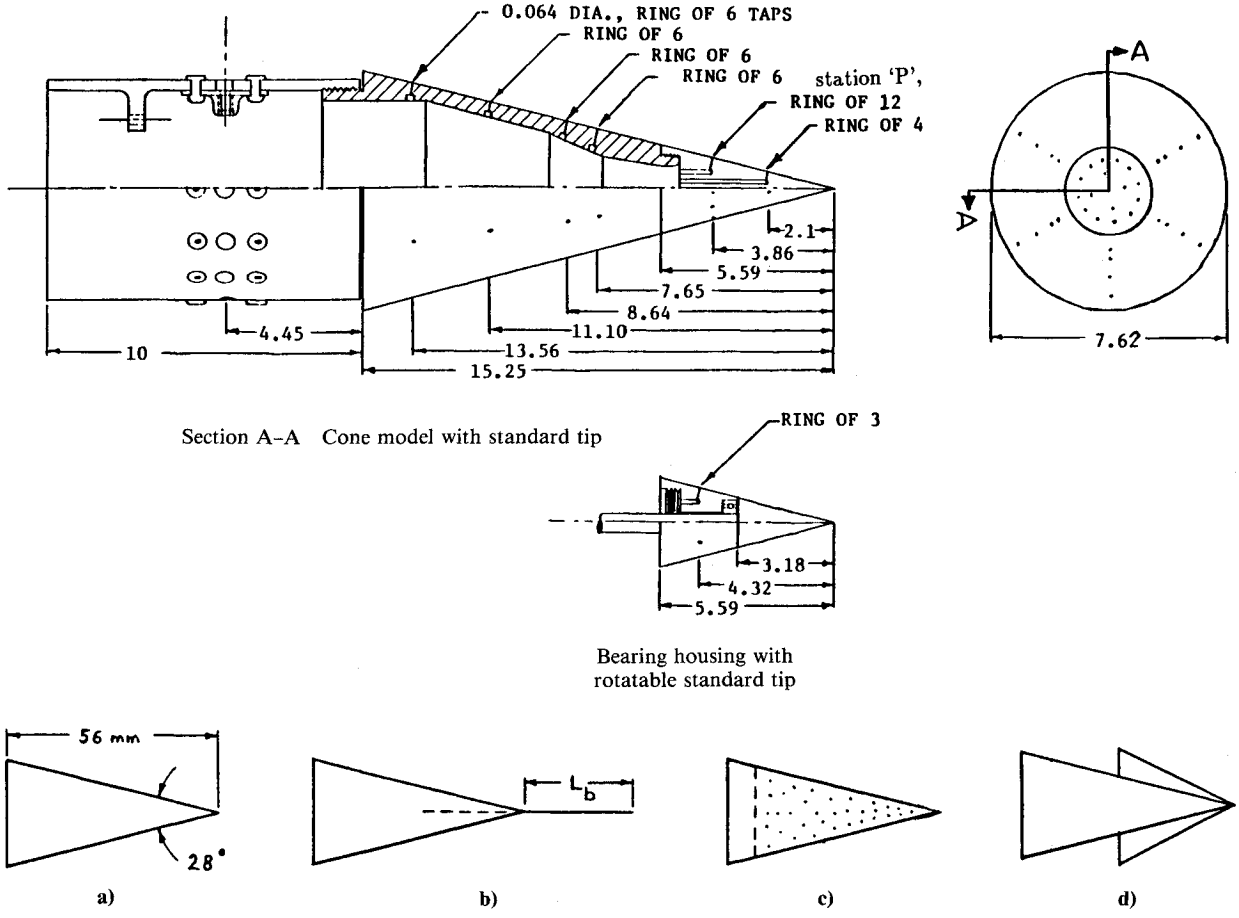

Fig. 2 Schematic diagrams of the cone model and tip geometries investigated in the present experimental program. All dimensions are in centimeters unless otherwise noted: a) standard, b) nose boom, c) porous, and d) delta strake.

Wind-Tunnel Tests

The models were tested in a closed-circuit laminar flow tunnel with a test section of 0.69 × 0.91 × 2.44 m. The tunnel was able to produce a stable flow with the speed ranging from 0.3 to 30 m/s at a turbulence level of less than 0.1%. The rectangular cross section, 0.69 × 0.91 m, was provided with 45-deg corner fillets that vary from 15.25 × 15.25 cm to 12.1 × 12.1 cm to partially compensate for the boundary-layer growth. The air speed was measured by a Betz manometer with an accuracy of 0.02 mm of water. Spatial variation of the mean velocity in the test section was observed to be less than 0.24%. Figure 3 shows an outline of the wind tunnel and the model support system. It may be pointed out that the model, supported on a six component strain-gauge balance, can be given any desired pitch attitude in the range ±90 deg. The yaw attitude can be varied over the range ±30 deg. The roll maneuver can be accomplished over the entire 360-deg range.

III. Results and Discussion

The amount of information obtained through a systematic test program involving the basic model, add-on tip devices, and their combinations is rather extensive. For conciseness, only a few of the typical results useful in establishing trends are presented here. The standard cone-tip data are presented first, which serve as reference to assess relative effectiveness of other tip geometries. Typical results for the nose boom, delta strake, and porous tip follow. Finally, the effect of tip rotation is evaluated. Such carefully planned experiments with repeatable results, aimed at side force alleviation through adjustment of the tip geometry, are indeed scarce and should prove helpful in better understanding the complex phenomenon.

Standard Tip

Figure 4a shows typical pressure distribution plots, at a station 25.3% from the tip, for the standard cone in the angle of attack α range of 0–50 deg and at a roll angle ϕ of 0 deg. Also referred to as station *P*, it has the largest number of pressure taps (12) and hence was well suited for presentation of the pressure asymmetry data. Similar pressure plots for aft stations confirmed the general trend. The results were integrated over the cone surface to evaluate the side and normal force components. In general, the lift increases with an increase in the angle of attack. Note, in the range α = 0–30 deg, the circumferential pressure distribution at the station *P* is essentially symmetric about the axial vertical plane. The asymmetry appears at α = 40 deg, suggesting the presence of a side force. Figure 4b shows a similar asymmetric pressure distribution case for a roll angle of 300 deg, but now the side force is in the opposite direction. For the 12 roll positions tested, the side force at a given angle of attack changed direction without suggesting any trend (with respect to the roll angle). This is understandable as the boundary-layer instability is governed by the tip surface roughness, a random parameter, besides other variables.

Figure 5 presents the side force variations for 12 different roll positions. It clearly shows a large increase in the side force starting at α close to 30 deg. This is approximately the value of the cone angle. It is apparent that the side force changes direction rather randomly as explained before. Its magnitude for a given α is also affected, perhaps due to the extent of asymmetry in the flow, induced by the surface roughness at the tip and other geometric perturbations.

Results when replotted to depict variation of the side force with roll angle for a fixed value of α led to the same conclusion. It should be recognized that although the forebody

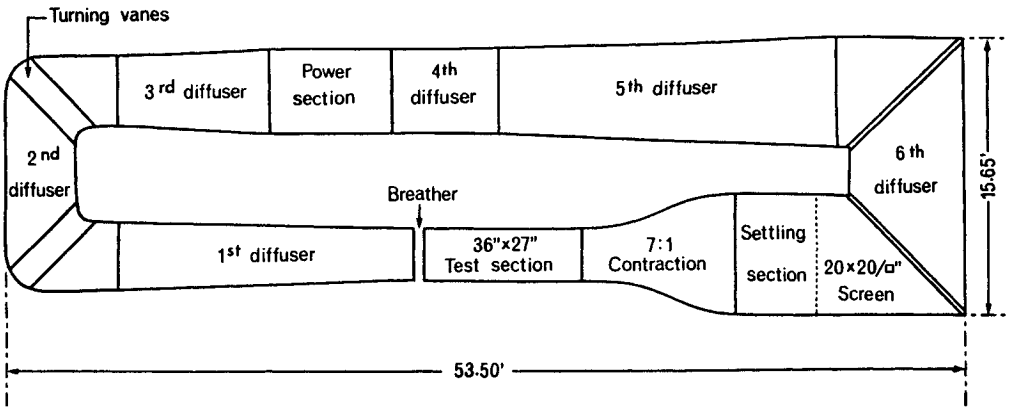

a)

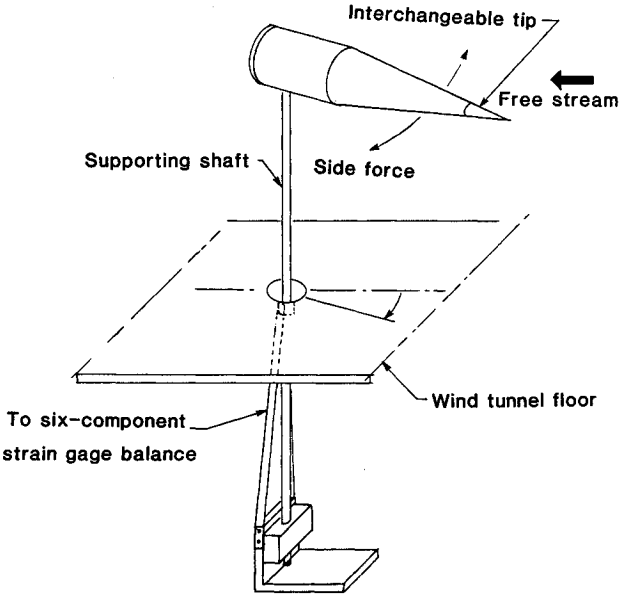

b)

Fig. 3 Schematic diagrams showing a) wind tunnel used in the test program, and b) model support system.

causes the flow asymmetry, the side force is contributed by the entire body, i.e., the base as well as the forebody.

Tip with a Nose Boom

For the nose-boom test, a family of nine 0.89-mm-diam tapered darning needles, varying in length L_b from 4.13 to 0.16 cm, was used. Each test with a nose boom was carried out at six roll positions. A marked dependence on the tip roll orientation continued to be present at higher angles of attack ($\alpha > 30$ deg), similar to that observed with the standard tip. The magnitude of the maximum side force did show a significant (50%) reduction (Fig. 6). Of course, tripping of the boundary layer due to presence of the boom can affect the side force; however, precise mechanism of its reduction is still not clearly understood.

Delta Strake Tip

Tests with a 3.18-cm delta strake tip were conducted at six different roll positions. Of primary interest was the effect of the strake when perpendicular to the pitch plane, as this configuration was expected to be successful at minimizing the side force. However, the tests were also conducted at roll angles of ± 10, ± 20, and ± 90 deg. The small roll angles would be of interest for noncoordinated flight maneuvers, whereas the 90-deg position was tried to compare its effectiveness in side force alleviation with the more conventional orientations of the strake.

Results of the side force variation with pitch and roll attitudes for the 3.18-cm delta strake are presented in Fig. 7a. Note, both the 0- and 90-deg roll orientations of the strake seem to promote symmetric flowfields with the 0 position proving a little better. For a given pitch angle, particularly $\geq$ 30 deg, the presence of a roll angle (± 10 deg, ± 20 deg) seems to reduce effectiveness of the strake in promoting the flow symmetry. However, it is encouraging that the side force remains relatively low over the entire range of the pitch angle tested.

It is important to point out that all of the strake tips larger than 0.32 cm (i.e., $L_S/L > 0.02$) showed promise in terms of the side force reduction. On the whole they performed much better than the nose booms. The maximum reduction in the side force coefficient achieved was around 88% of the nominal value with the delta strake of $L_s = 3.19$ cm ($L_S/L = 0.21$, Fig. 7b).

Porous Tip

The porous brass tip used in the test program was equipped with a 3.18-cm nose boom and perforated with 0.64-mm holes. The perforated portion composed approximately 20% of the total cone length. The maximum recorded side force coefficient was 0.62, a 38% reduction from the nose-boom case and a 49% reduction from the standard tip value. On the other hand, the porous tip recorded a slightly higher (6%) normal force than that with the standard tip.

It seems logical that an efficient porous tip with near instantaneous communication of pressure across its surface would enhance symmetric vortex formation as well as negate the effects of asymmetric vortices. Unfortunately, the porous tip used in the present test program had several limitations:

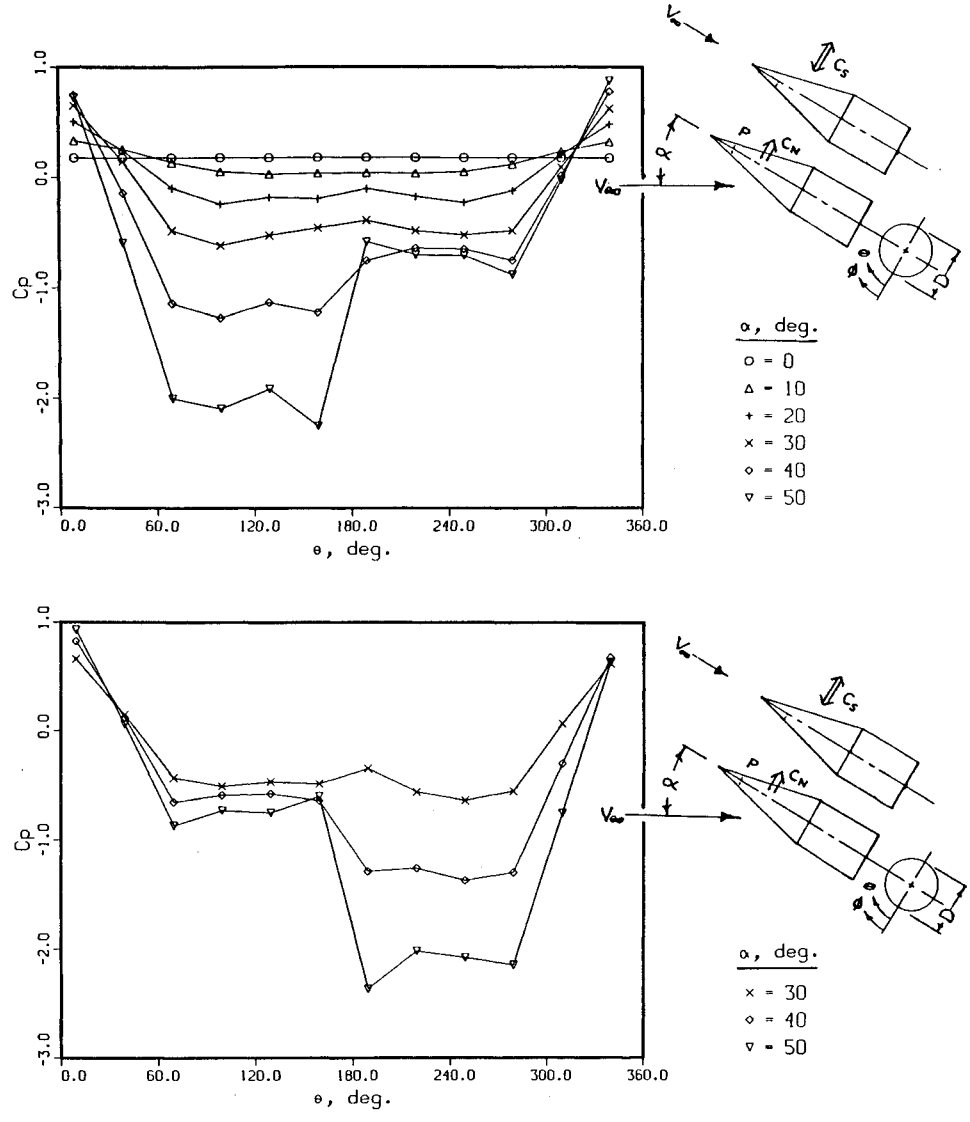

Fig. 4 Pressure distribution at a reference station *P*, as affected by the angle of attack α, for the standard tip: a) roll angle $\phi = 0$ deg, and b) roll angle $\phi = 300$ deg.

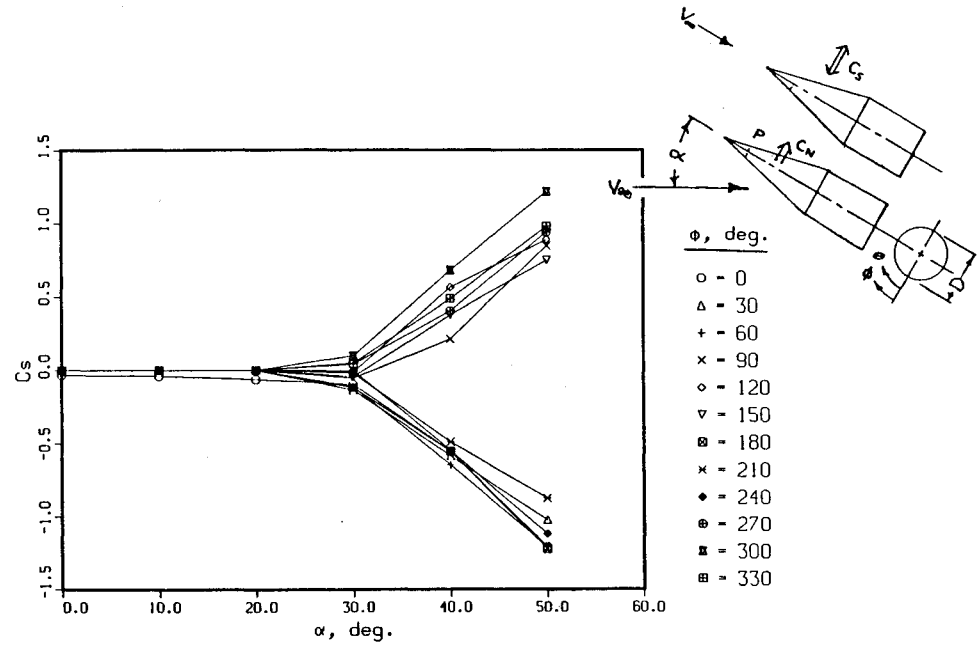

Fig. 5 Variation of the side force coefficient for the standard tip model, with pitch α and roll ϕ.

1) The tap size is rather large, contributing to the surface roughness, thus partly canceling its desired influence.

2) The porous length is perhaps too long, thus presenting a larger internal volume resulting in the average pressure that is different from the local value.

3) The problem in limitation 2 is further accentuated here as the internal gap extends to the base of the cone and communicates with the pressure there.

However, the effectiveness of the porous tip in reducing the side force is clearly established, even by this preliminary test. Better planned experiments in this direction are likely to be fruitful.

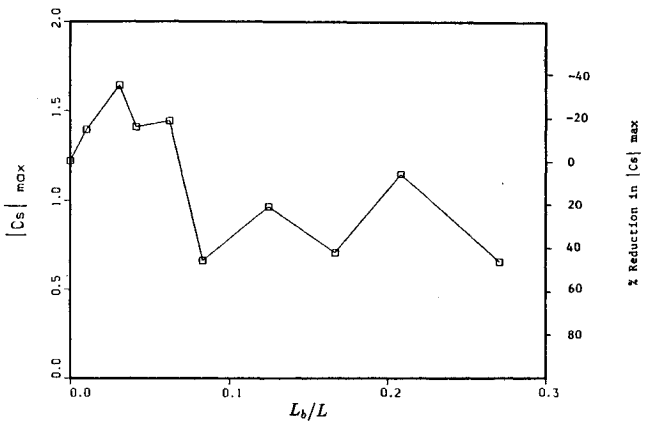

Fig. 6 Magnitude of the maximum side force coefficient and its percentage reduction as affected by the nose-boom length. Result for the standard tip is also included to facilitate comparison.

Spinning Tip

The earlier preliminary investigation by Modi et al.[1] had suggested a possible reduction in the side force when the tip of the cone was spun. Several carefully planned tests were conducted to assess more precisely the effect of tip rotation. The first set of tests involved spinning the standard tip and the nose booms of up to 1.27 cm in length. All of these tests were conducted at 2000 rpm, the maximum speed of the small dc motor used. Variations in the side force with the pitch angle are shown in Fig. 8a. For each tip tested, the model was pitched through 50 deg and the test repeated with the spin reversed. Two observations of interest can be made:

1) The direction of the spin determines the direction of the side force. A clockwise rotation leads to a net left side force (as viewed by the pilot). The opposite is true for the anticlockwise spin. This is in agreement with the results of Ericsson and Reding.[22]

2) The tip rotation can lead to a significant reduction in the side force. Figure 8b demonstrates the effectiveness of various nose booms in reducing the side force at 2000 rpm.

These results show that reduction in the range of 50–75% of the nominal value can be obtained by spinning the tip with a nose boom. The maximum side force reduction, with a 0.318-cm nose-boom tip spinning at 2000 rpm, was around 25% of the nominal value. Note that the same boom length in the non-spinning tests actually increased the side force from the nominal value. It is interesting to observe that the spinning standard tip is quite effective with the side force reduced by 71%.

The second set of tests involved spinning a 1.27-cm nose boom over a range of speeds. The side force variation with the pitch and the spin rate are shown in Fig. 9a. Again the sense of

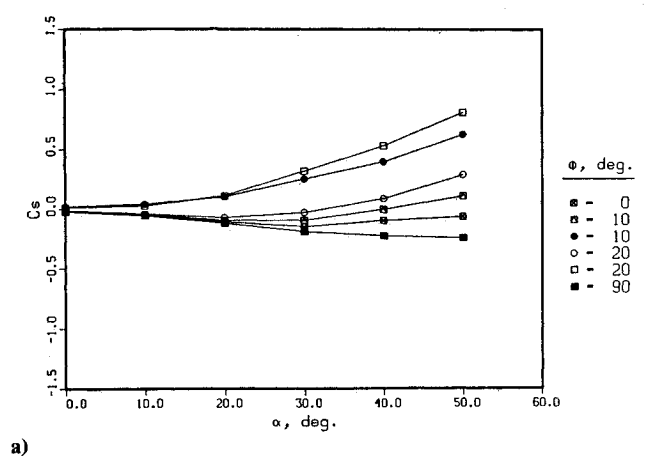

Fig. 7 Effect of delta strakes on the side force: a) variation of the side force coefficient with pitch and roll angles for a 3.18-cm span (aspect ratio 2) strake, and b) effect of the strake length (aspect ratio 2) on the magnitude of the side force.

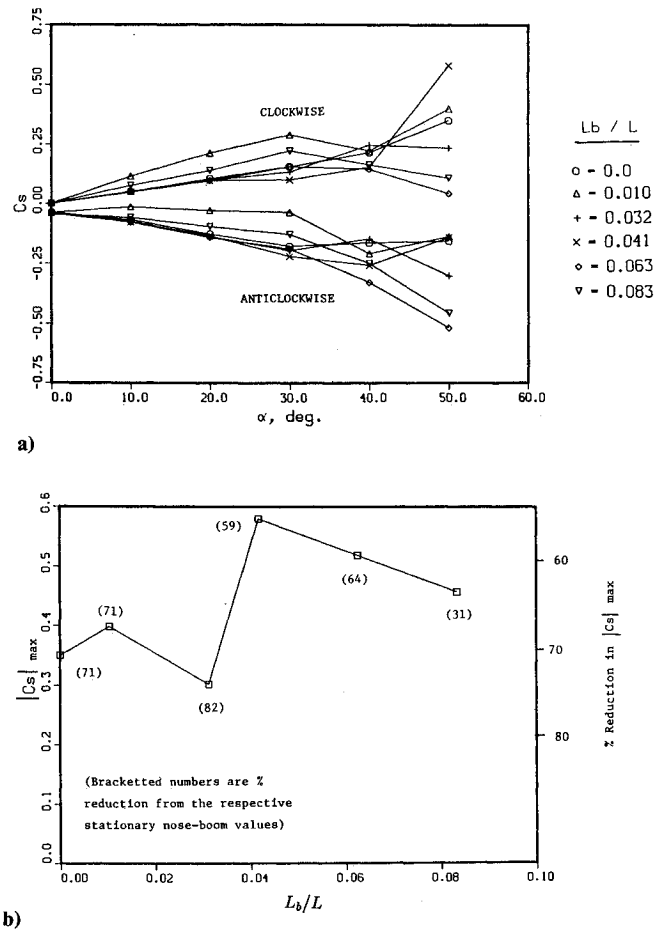

Fig. 8 Effect of tip rotation on the side force: a) side force variation as affected by the pitch angle and nose-boom length at a tip spin rate of 2000 rpm, and b) reduction in the maximum side force as a function of the boom length at 2000 rpm.

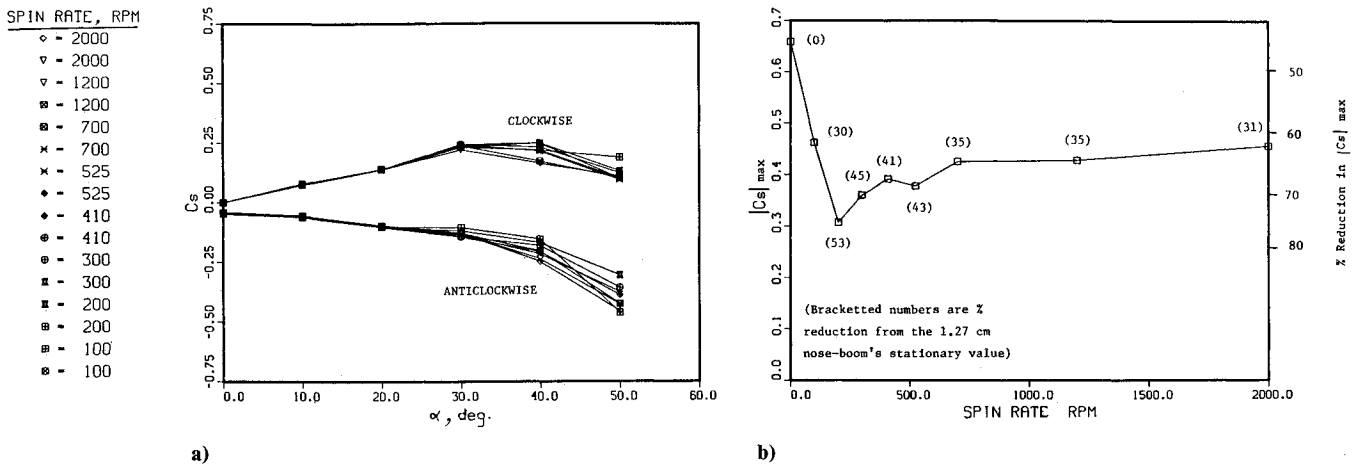

a) b)

Fig. 9 Effect of tip rotation with a 1.27-cm nose boom: a) side force variation as affected by the pitch angle and spin rate, and b) reduction in the maximum side force as a function of tip speed.

rotation has determined the side force direction. With the present motor, it was not possible to obtain a stable spin rate below 100 rpm.

Figure 9b shows the maximum side force variation with spin rate for 1.27-cm nose boom. Note a clear minimum in the side force at 200 rpm. In fact, any spin rate seems to reduce the side force with 200 rpm yielding 25% of the nominal value and 46% of the zero spin case, for the same tip. Investigations by other researchers[1,22] suggest that the maximum reduction in the side force occurs at a spin rate in the range of 100–400 rpm.

As can be expected, for all the spin tests, results were independent of the initial roll angle.

IV. Concluding Remarks

The subject of vortex-dominated flows has proven to be far more complex than the first impressions would indicate. As often happens in investigations of aerodynamic phenomena, many uncontrollable parameters appear that not only complicate but also sometimes invalidate the test results.

The carefully planned experiments with repeatable results have given, for the first time, reliable information concerning effectiveness of several tip geometries on the side force reduction. The tests with a 28-deg cone-cylinder model, provided with the standard tip, nose booms without and with porous apex, delta strakes, and tip rotation, yielded fundamental information leading to a better appreciation of the complex flow. Based on the results, it can be concluded that modifications of the tip geometry and their judicious combinations can lead to a substantial reduction in the side force. Such passive procedures for the side force control are indeed quite attractive; however, considerable scope for further study exists to arrive at an optimum configuration. Numerical prediction of the side force for a pointed forebody at high angles of attack is a formidable problem in itself. The presence of tip devices would add to the challenge. There is a considerable scope for innovation in this general area pertaining to separated flows at high angles of attack.

Acknowledgment

This investigation was supported by the Natural Sciences and Engineering Research Council of Canada, Grant A-2181.

References

[1]Modi, V. J., Ries, T., Kwan, A., and Leung, E., "Aerodynamics of Pointed Forebodies at High Angles of Attack," *Journal of Aircraft,* Vol. 21, No. 6, 1984, pp. 428–432.

[2]Ericsson, L. E., and Reding, J. P., "Vortex Induced Asymmetric Loads in 2-D and 3-D Flows," AIAA 18th Aerospace Sciences Meeting, AIAA Paper 80-0181, Pasadena, CA, Jan. 1980.

[3]Ericsson, L. E., and Reding, J. P., "Alleviation of Vortex Induced Asymmetric Loads," *Journal of Spacecraft and Rockets,* Vol. 17, No. 6, 1980, pp. 546–553.

[4]Reding, J. P., and Ericsson, L. E., "Maximum Vortex-Induced Side Force Revisited," AIAA 21st Aerospace Sciences Meeting, AIAA Paper 83-0458, Reno, NV, Jan. 1983.

[5]Stewart, A. C., "An Experimental Investigation of the Pointed Forebody Aerodynamics," M.A.Sc. Thesis, Dept. of Mechanical Engineering, Univ. of British Columbia, Vancouver, B.C., Canada, Aug. 1988.

[6]Moskovitz, C. A., Hall, R. M., and DeJarnette, F. R., "Effects of Nose Bluntness, Roughness and Surface Perturbations on the Asymmetric Flow Past Slender Bodies of Large Angles of Attack," AIAA 7th Applied Aerodynamics Conference, AIAA Paper 89-2236, Seattle, WA, July/Aug. 1989.

[7]Moskovitz, C. A., Hall, R. M., and DeJarnette, F. R., "Experimental Investigation of a New Device to Control the Asymmetric Flowfield on Forebodies at Large Angles of Attack," AIAA 28th Aerospace Sciences Meeting, AIAA Paper 90-0069, Reno, NV, Jan. 1990.

[8]Tavella, D. A., Schiff, L. B., and Cummings, R. M., "Pneumatic Vortical Flow Control at High Angles of Attack," AIAA 28th Aerospace Sciences Meeting, AIAA Paper 90-0098, Reno, NV, Jan. 1990.

[9]Hoang, N. T., Telionis, D. T., and Jones, G. S., "The Hemisphere-Cylinder at an Angle of Attack," AIAA 28th Aerospace Sciences Meeting, AIAA Paper 90-0050, Reno, NV, Jan. 1990.

[10]Blake, W. B., and Barnhart, B. P., "Rotational Aerodynamics of Elliptic Bodies at High Angles of Attack," AIAA 28th Aerospace Sciences Meeting, AIAA Paper 90-0068, Reno, NV, Jan. 1990.

[11]Zilliac, G. G., Degani, D., and Tobak, M., "Asymmetric Vortices on a Slender Body of Revolution," AIAA 28th Aerospace Sciences Meeting, AIAA Paper 90-0388, Reno, NV, Jan. 1990.

[12]Hartwich, P. M., Hall, R. M., and Hemsch, M., "Navier-Stokes Computations of Vortex Asymmetries Controlled by Small Surface Imperfections," AIAA 28th Aerospace Sciences Meeting, AIAA Paper 90-0385, Reno, NV, Jan. 1990.

[13]Cebeci, T., McIlvaine, M., Chent, M. M., and Liebeck, R. H., "Calculation of Low Reynolds Number Flow at High Angles of Attack," AIAA 28th Aerospace Sciences Meeting, AIAA Paper 90-0569, Reno, NV, Jan. 1990.

[14]Kandil, O. A., Wong, T. C., and Liu, C. H., "Prediction of Steady and Unsteady Asymmetric Vortical Flow Around Cones," AIAA 28th Aerospace Sciences Meeting, AIAA Paper 90-0598, Reno, NV, Jan. 1990.

[15]Degani, D., Schiff, L. B., and Levy, Y., "Physical Considerations Governing Computation of Turbulent Flows Over Bodies at Large Incidence," AIAA 28th Aerospace Sciences Meeting, AIAA Paper 90-0096, Reno, NV, Jan. 1990.

[16]Verhaagen, N. G., and van Ransbeeck, P. R. O., "Experimental and Numerical Investigation of the Flow in the Core of a Leading Edge Vortex," AIAA 28th Aerospace Sciences Meeting, AIAA Paper 90-0384, Reno, NV, Jan. 1990.

[17]Ng, T. T., "Aerodynamic Control of NASP-Type Vehicles Through Vortex Manipulation," AIAA 28th Aerospace Sciences

Meeting, AIAA Paper 90-0594, Reno, NV, Jan. 1990.
[18]Del Frate, J. H., and Zuniga, F. A., "In-Flight Flow Field Analysis of the NASA F-18 High Alpha Research Vehicle with Comparisons to Ground Facility Data," AIAA 28th Aerospace Sciences Meeting, AIAA Paper 90-0231, Reno, NV, Jan. 1990.
[19]Rao, D. M., "Side-Force Alleviation on Slender, Pointed Forebodies at High Angles of Attack," *Journal of Aircraft,* Vol. 16, No. 11, 1979, pp. 763–768.
[20]Skow, A. M., Moore, W. A., and Lorincz, D. J., "Control of Forebody Vortex Orientation to Entrance Departure Recovery of Fighter Aircraft," *Journal of Aircraft,* Vol. 19, No. 10, 1982, pp. 812–819.
[21]Peake, D. J., Owen, F. K., and Johnson, D. A., "Control of Forebody Vortex Orientation to Alleviate Side Forces," AIAA 18th Aerospace Sciences Meeting, AIAA Paper 80-0183, Pasadena, CA, Jan. 1980.
[22]Ericsson, L. E., and Reding, J. P., "Dynamics of Forebody Flow Separation and Associated Vortices," AIAA Atmospheric Flight Mechanics Conference, AIAA Paper 83-2118, Gatlinburg, TN, Aug. 1983.